universe

MDPI

Article

Resonant Effect of High-Energy Electron–Positron Pairs Production in Collision of Ultrarelativistic Electrons with an X-ray Electromagnetic Wave

Georgii K. Sizykh *, Sergei P. Roshchupkin and Victor V. Dubov

Department of Theoretical Physics, Peter the Great St. Petersburg Polytechnic University, Polytechnicheskaya 29, 195251 Saint Petersburg, Russia; roshchupkin_s@spbstu.ru (S.P.R.); dubov@spbstu.ru (V.V.D.)

* Correspondence: georgiisizykh@yandex.ru

Abstract: The process of resonant high-energy electron–positron pairs production by electrons in an X-ray pulsar electromagnetic field is studied theoretically. Under the resonance conditions, the second-order process under consideration effectively reduces into two sequential first-order processes: X-ray-stimulated Compton effect and X-ray–stimulated Breit–Wheeler process. The kinematics of the process is studied in detail: the dependencies of the energy of the scattered electron on its outgoing angle and the energies of the particles of the pair on the outgoing angle of the scattered electron and the opening angle of the pair are obtained. The analysis of the number of different possible particles energies values in the entire range of the angles is also carried out, according to which the energies of the particles of the pair can take up to eight different values at a fixed outgoing angle of the scattered electron and opening angle of the pair. The estimate of the resonant differential probability per unit time of the process, which reaches the maximum value of 24 orders of the value of the non-resonant differential probability per unit time, is obtained. The angular distribution of the differential probability per unit time of the process is analyzed, particularly for the case of high-energy positrons presenting in pulsar radiation.

Keywords: external field QED; high-energy particle physics; resonances; Oleinik resonances; trident pair production; ultrarelativistic particles; electron; positron; kinematics; X-ray pulsar

PACS: 95.30.Cq; 97.10.Ld; 97.80.Jp

Citation: Sizykh, G.K.; Roshchupkin, S.P.; Dubov, V.V. Resonant Effect of High-Energy Electron–Positron Pairs Production in Collision of Ultrarelativistic Electrons with an X-ray Electromagnetic Wave. *Universe* **2021**, *7*, 210. https://doi.org/10.3390/universe7070210

Academic Editor: Maria Vasileiou

Received: 23 May 2021
Accepted: 20 June 2021
Published: 24 June 2021

1. Introduction

Oleinik resonances [1,2] (see also reviews [3,4]) have been studied for quite a long time. The peculiarity of the resonant processes of quantum electrodynamics (QED) is the large value of the differential probability of such processes. However, for the resonant processes to take place, an additional connection between the 4-momenta of the interacting particles is necessary, which leads to stricter functional dependencies of the energies of the outgoing particles on the angles. Since the works of Oleinik, various resonant processes of quantum electrodynamics in an external electromagnetic field have been considered from different angles (see, for example, [5–26]). Thus, in the monograph [5], the first-order external field QED processes into which higher-order processes reduce in resonance are studied in detail and in the works [6–26], the resonant second-order external field QED processes are studied.

Recently, anomalous high-energy positron abundance [27] was discovered in cosmic rays. It has been suggested that the positrons were produced by pulsars [28]. The mechanism is a particle-antiparticle pair production in the electromagnetic field of a pulsar. One of the purposes of our article is to answer if the explanation suggested in the work [28] may or may not be implemented in this case. We conclude that the positrons discussed

may be produced by pulsars, in particular, in the process of resonant electron-positron pair production in collision of an electron with the electromagnetic field of a pulsar.

The process of electron–positron pairs production in collision of electrons with an electromagnetic wave (also non-linear trident pair production, NTPP) was studied in [29–34]. In [29], the main attention is paid to the process amplitude, which reduces into the sum of resonant and non-resonant process amplitudes. The authors also give numerical estimates of the probability of the process in the intense field of a plane electromagnetic wave. In [30], authors investigate this process in a pulse field with an arbitrary envelope and obtain expressions for the probability of the process, including for the interference terms, and also numerically calculate the probability of the process. In [31], authors also study the NTPP process in a strong laser field and aim to try to describe the SLAC experiment [32] where a nonlinear Compton effect was studied. In [33], the NTPP process in a strong laser field is investigated. Special attention is paid to separation of contributions of resonant and non-resonant processes. In [34], authors study this process in a constant-crossed field background. Contributions to the probability of resonant and nonresonant processes are also investigated. The NTPP process was also studied in [23], but resonant kinematics of the process was not studied in sufficient detail, and only an estimate of the resonant differential probability was given.

In contrast to the previous article [23], the resonant kinematics of the process in the X-ray field is studied in detail, taking into account different energies of initial ultrarelativistic electrons, as well as different possible energies of electron–positron pairs and scattered electrons. An estimate for the differential probability per unit time of the process is given and the angular probability distribution is investigated.

We will model an external electromagnetic field as a plane monochromatic circularly polarized electromagnetic wave propagating along the z-axis, with a 4-potential

$$A(\varphi) = \frac{F}{\omega}\left(e_x \cos\varphi + \delta e_y \sin\varphi\right), \quad \varphi = kx = \omega(t - z), \tag{1}$$

where ω and F are the frequency and the electric field strength of the wave, e_x and e_y are polarization 4-vectors, $\delta = \pm 1$, $k = (\omega, \boldsymbol{k})$ is light wave 4-momentum and $x = (t, \boldsymbol{x})$ is 4-radius-vector.

In this problem, the main parameter is the classical relativistically invariant parameter

$$\eta = \frac{eF\lambda\!\!\!^{-}}{mc^2}, \tag{2}$$

the physical meaning of which is the ratio of the work of electromagnetic field at its wavelength to an electron (positron) rest energy. Here e and m are the elementary charge and the mass of an electron (positron), $\lambda\!\!\!^{-}$ is the reduced wavelength of the field and c is the speed of light. This paper is devoted to resonant kinematics in a weak circularly polarized X-ray pulsar field, which corresponds to the value of the parameter η:

$$\eta \ll 1. \tag{3}$$

In Section 2, we study the amplitude of the process in the field of a weak circularly polarized electromagnetic wave. In Section 3, the resonant kinematics of the process is studied in detail: in Section 3.1, we obtain expressions for the energies of the scattered electron and the particles of the pair as a function of the angle of departure of the scattered electron and the opening angle of the pair, in Sections 3.2–3.4, the restrictions on the angles and energies of the particles are studied in detail. In Section 4, the expression is given for the resonant differential probability per unit time of the process and the angular dependence of the probability is discussed. The conclusion is made in Section 5.

Further we use relativistic system of units: $\hbar = c = 1$.

2. Process Amplitude

The process of resonant electron–positron pairs production in collision of ultrarelativistic electrons with an X-ray pulsar wave in the second order of perturbation theory is described by two Feynman diagrams (see Figure 1).

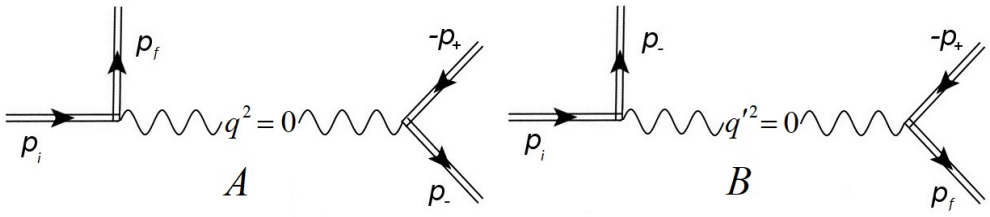

Figure 1. Feynman diagrams of the process of electron–positron pairs production when electrons collide with the field of an X-ray pulsar. The solid lines correspond to the Volkov functions of the initial and scattered electrons with 4-momenta p_i and p_f and to the particles of the pair with 4-momenta $p_\pm$, the wavy lines correspond to the intermediate photons. Channels A and B are distinguished by replacement of electrons states $\left(p_f \Longleftrightarrow p_-\right)$.

The amplitude of the process is obtained by standard methods [35] and can be reduced to the form [23]:

$$S = \sum_{l=2}^{\infty} S_l, \tag{4}$$

where S_l are partial amplitudes corresponding to l photons of external field absorbed in the process and given by the following expression:

$$\begin{gathered} S_l = 16\pi^5\alpha \frac{e^{-id^*}}{\sqrt{E_i E_f E_- E_+}} M_l \delta^{(4)}\left(p_i - p_f - p_+ - p_- + lk\right) - \left(p_f \longleftrightarrow p_-\right), \\ M_l = \sum_{r'=1}^{\infty} \frac{\left[\overline{u}_{p_-} H_{\mu;-r'} v_{-p_+}\right]\left[\overline{u}_{p_f} H'^{\mu}_{-(l-r')} u_{p_i}\right]}{\left(p_+ + p_- - r'k\right)^2}, \end{gathered} \tag{5}$$

where d^* is an independent of the summation index phase, $p_{i,f} = (E_{i,f}, \boldsymbol{p}_{i,f})$ are the initial and scattered electrons 4-momenta, $p_\pm = (E_\pm, \boldsymbol{p}_\pm)$ are the 4-momenta of the particles of the pair. In Equation (5) u_{p_i}, $\overline{u}_{p_-}$, $\overline{u}_{p_f}$ and v_{-p_+} are free Dirac bispinors, $\gamma_\mu (\mu = 0,1,2,3)$ are Dirac γ-matricies, hats denote scalar product of a vector and the vector $\gamma_\mu (e.g., \hat{k} = k_0\gamma_0 - k_1\gamma_1 - k_2\gamma_2 - k_3\gamma_3)$ and

$$H^{\mu}_n = \gamma^\mu L_n\left(\gamma_{p_+p_-}, \chi_{p_+p_-}\right) + b^{\mu}_- L_{n-1}\left(\gamma_{p_+p_-}, \chi_{p_+p_-}\right) + b^{\mu}_+ L_{n+1}\left(\gamma_{p_+p_-}, \chi_{p_+p_-}\right), \tag{6}$$

$$H'^{\mu}_n = \gamma^\mu L_n\left(\gamma_{p_ip_f}, \chi_{p_ip_f}\right) + b'^{\mu}_- L_{n-1}\left(\gamma_{p_ip_f}, \chi_{p_ip_f}\right) + b'^{\mu}_+ L_{n+1}\left(\gamma_{p_ip_f}, \chi_{p_ip_f}\right). \tag{7}$$

where

$$b^{\mu}_\pm = \eta\left[\frac{m}{4(kp_-)}\hat{\varepsilon}_\pm\hat{k}\gamma^\mu - \frac{m}{4(kp_+)}\gamma^\mu\hat{k}\hat{\varepsilon}_\pm\right], \quad b'^{\mu}_\pm = \eta\left[\frac{m}{4(kp_i)}\gamma^\mu\hat{k}\hat{\varepsilon}_\pm + \frac{m}{4\left(kp_f\right)}\hat{\varepsilon}_\pm\hat{k}\gamma^\mu\right], \tag{8}$$

$$\varepsilon_\pm = e_x \pm i\delta e_y$$

and in case of circular polarization $(\delta = \pm 1)$ special functions L take the following form (see [36]):

$$L_n\left(\gamma_{pp'}, \chi_{pp'}\right) = e^{-il\chi_{pp'}} J_n\left(\gamma_{pp'}\right), \tag{9}$$

where $J_n\left(\gamma_{pp'}\right)$ is the Bessel function of the integer index. The L-functions have arguments of the following form:

$$\gamma_{pp'} = \eta m\sqrt{-Q^2_{pp'}}, \qquad \mathrm{tg}\chi_{pp'} = \frac{\left(Q_{pp'}e_y\right)}{\left(Q_{pp'}e_x\right)}, \qquad Q_{pp'} = \frac{p}{(kp)} - \frac{p'}{(kp')}, \tag{10}$$

which are defined by corresponding expressions in the amplitudes (6) and (7).

3. Resonant Kinematics

In the plane monochromatic electromagnetic wave field, fermion states are described by the Volkov functions, for which the 4-momentum components are no longer good quantum numbers. Instead, the components of the 4-quasi-momentum are conserved, which, however, in the case of weak fields (3) differ slightly from the components of the ordinary 4-momentum, so the 4-momentum conservation law is approximately fulfilled. It also should be noted that in a weak field, multiphoton processes are suppressed, so we will study the process with the absorption of only one photon at each vertex.

We will consider an ultrarelativistic initial electron (and, as a consequence, ultrarelativistic outgoing particles):

$$E_{i,f,\pm} \gg m. \tag{11}$$

This case is interesting, because due to the high energy of the initial electron, the requirements for the field intensity for generation of electron–positron pairs are reduced. The requirement of ultrarelativistic particles leads to the fact that all particles propagate in a narrow cone along the direction of motion of the initial electron, which must also lie far from the direction of the wave vector of an external field:

$$\theta_{fi} = \angle\left(\boldsymbol{p}_i, \boldsymbol{p}_f\right) \ll 1, \quad \theta_{\pm} = \angle\left(\boldsymbol{p}_+, \boldsymbol{p}_-\right) \ll 1, \quad \theta_{i,f,\pm} = \angle\left(\boldsymbol{p}_{i,f,\pm}, \boldsymbol{k}\right) \sim 1. \tag{12}$$

Further, we study the kinematics of the channel A. The kinematics of the channel B is obtained from it by simply replacing the indices: $\left(p_f \longleftrightarrow p_-\right)$.

In the first vertex, under resonance conditions the X-ray-stimulated Compton effect takes place. In this case, we have the 4-momentum conservation law in the form

$$p_i + k = p_f + q, \tag{13}$$

which, combined with the resonance condition,

$$q^2 = 0 \tag{14}$$

leads to the equation on the scattered electron energy

$$x_f^2\left(1 + 4\varepsilon_i + 4\varepsilon_i^2\delta_{fi}^2\right) - 2(1 + 2\varepsilon_i)x_f + 1 = 0. \tag{15}$$

In Equation (15) the following notations are introduced:

$$x_f = \frac{E_f}{E_i}, \quad \varepsilon_i = \frac{E_i}{\omega_{thr}}, \quad \omega_{thr} = \frac{m^2}{\omega \sin^2\theta_i/2}, \quad \delta_{fi}^2 = \frac{\omega_{thr}^2\theta_{fi}^2}{4m^2}. \tag{16}$$

In Notations (16) x_f is the energy of scattered electron in units of the energy of the initial electron, ω_{thr} is the threshold energy in the X-ray-stimulated Breit–Wheeler process, ε_i is the energy of the initial electron in units of the X-ray-stimulated Breit–Wheeler process threshold energy ω_{thr} (see the text after the Expression (22)), and δ_{fi} is normalized angle between the scattered and the initial electron propagation directions.

The solutions of Equation (15) are given as follows

$$x_{f(1,2)} = \frac{1 + 2\varepsilon_i \pm 2\varepsilon_i\sqrt{(1 - \delta_{fi}^2)}}{1 + 4\varepsilon_i + 4\varepsilon_i^2\delta_{fi}^2}, \tag{17}$$

where $x_{f(1)}$ corresponds to "+" sign before square root and $x_{f(2)}$—to "−" sign.

It could be seen from Expression (17) that for fixed value of the outgoing angle the scattered electron can have one of the two possible energies.

It should also be noted that there is an upper bound on the value of the outgoing angle of the scattered electron:

$$\delta_{fi}^2 \leq 1. \tag{18}$$

In the second vertex (see Figure 1), the X-ray-stimulated Breit–Wheeler process takes place. In this case, the 4-momentum conservation law

$$q + k = p_- + p_+ \tag{19}$$

along with the resonance condition (14) and approximate energy conservation law

$$1 \approx x_f + x_+ + x_-, \quad x_\pm = E_\pm / E_i \tag{20}$$

leads to the equation on the energy of the positron of the pair:

$$4\varepsilon_i^2\delta_{+-}^2 x_+^4 - 8\varepsilon_i^2\delta_{+-}^2\Big(1-x_f\Big)x_+^3 + \Big[4\varepsilon_i(1-x_f) + 4\varepsilon_i^2\delta_{+-}^2(1-x_f)^2\Big]x_+^2 - 4\varepsilon_i(1-x_f)^2 x_+ + (1-x_f)^2 = 0. \tag{21}$$

In Equation (21)

$$\delta_{+-}^2 = \frac{\omega_{thr}^2\theta_{+-}^2}{4m^2}. \tag{22}$$

It also should be noted that fulfilling of 4-momentum conservation law (19) and resonance condition (14) leads to the presence of the threshold energy for the intermediate photon (see Expression (16)).

Equation (21) reduces to a biquadrate equation and has the following solutions.

$$x_{+(1,2,3,4)} = \frac{(1-x_f)}{2}\left(1 \pm \sqrt{1 - 2\frac{1 \pm \sqrt{1-\delta_{+-}^2}}{\varepsilon_i\delta_{+-}^2(1-x_f)}}\right), \tag{23}$$

where $x_{+(1)}$ corresponds to "+", "+" signs, $x_{+(2)}$—to "+", "−", $x_{+(3)}$—to "−", "+", $x_{+(4)}$—to "−", "−". From the Expression (23), one can see that the positron energy can take one of four different values at fixed pair opening angle and scattered electron energy. Taking into account the fact that scattered electron can have one of two possible energies—$x_{f(1)}$ and $x_{f(2)}$—it turns out that at fixed opening angle of the pair and outgoing angle of the scattered electron, the positron energy can take up to eight different values.

We also can find the electron of the pair energy from the energy conservation law (20):

$$x_{-(1,2,3,4)} = \frac{(1-x_f)}{2}\left(1 \mp \sqrt{1 - 2\frac{1 \pm \sqrt{1-\delta_{+-}^2}}{\varepsilon_i\delta_{+-}^2(1-x_f)}}\right), \tag{24}$$

where the choice of signs is determined in the same way as for the positron, that is, for example, $x_{-(1)}$ corresponds to the choice of signs "+", "+". The choice of signs in Expressions (23) and (24) must be done in such a way that the energy conservation law (20) is fulfilled, that is, before the external roots, the signs in the expressions for the energies of the particles of the pair must differ, and—before the internal roots—coincide. For example, if the positron has the energy $x_{+(1)}$, then the electron of the pair has the energy $x_{-(3)}$, and vice versa. Similarly with the energies $x_{\pm(2)}$ and $x_{\pm(4)}$.

From the Expressions (23) and (24) immediately follows the restriction on the opening angle of the pair:

$$\delta_\pm^2 \leq 1. \tag{25}$$

Thus, in the X-ray-stimulated Breit–Wheeler process, the particles of the pair can have up to four possible energy values for a certain opening angle of the pair and at a fixed energy of the scattered electron, which gives up to eight values of the energies of the particles of the pair at fixed outgoing angle of the scattered electron and opening angle of the pair.

3.1. Scattered Electron Energy Bounds

The condition for the existence of Solutions (23) imposes the following restriction on the process parameters:

$$1 - 2\frac{1 \pm \sqrt{1 - \delta_{+-}^2}}{\varepsilon_i \delta_{+-}^2 (1 - x_f)} \geq 0. \tag{26}$$

When selecting the "+ " sign (solutions $x_{\pm(1,3)}$) the Inequality (26) leads to a restriction on the energy of the scattered electron

$$x_f \leq x_{f;max}^{(1)}, \quad x_{f;max}^{(1)} = 1 - 2/\varepsilon_i, \tag{27}$$

and when selecting the "−" sign (solutions $x_{\pm(2,4)}$)—to a restriction

$$x_f \leq x_{f;max}^{(2)}, \quad x_{f;max}^{(2)} = 1 - 1/\varepsilon_i. \tag{28}$$

For better understanding of the Inequalities (27) and (28) one can have a look at Figure 2. As long as the energy of the scattered electron does not exceed the value $x_{f;max}^{(1)}$, all the eight possible solutions (four solutions for each of the two branches $x_{f(1,2)}$) for particles energies $x_{\pm(1,2,3,4)}$ are available. The possibility of their implementation is, of course, determined by specific values of the parameters δ_{fi}^2 and $\delta_{\pm}^2$. When the energy of the scattered electron lies in the interval $x_{f;max}^{(1)} \leq x_f \leq x_{f;max}^{(2)}$, the energies of the particles of the pair can take only four values (two solutions for each of the two solutions $x_{f(1,2)}$). If $x_f > x_{f;max}^{(2)}$, then the particles of the pair cannot have any energies allowed by the 4-momentum conservation law and the resonance condition, that is, such a case is not implemented in practice (we should emphasize that we are talking only about resonant processes!).

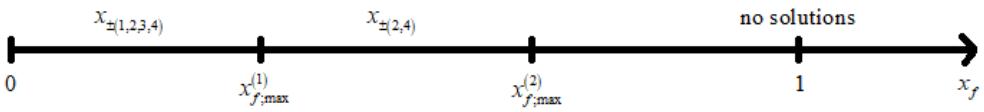

Figure 2. The regions of the scattered electron energy and the possible energies of the particles of the pair in these regions (see Inequalities (27) and (28)).

3.2. Initial Electron Energy Bounds

Further, we will discover four characteristic energies of the initial electron. The first of them we call the threshold energy and denote as ε_{thr}, since it has the meaning that at the energies of the initial electron less than this threshold energy, the studied process is impossible. The other three characteristic energies we denote $\varepsilon_1, \varepsilon_2$, and ε_3. The expressions for ε_{thr} and ε_1 were already obtained earlier (see formulas (23), (25) in [23]). Here, however, a more systematic approach to finding them is outlined, which also leads to appearance of the characteristic energies ε_2 and ε_3.

Next, we consider the Constraints (26) for different branches of the energy of the scattered electron—$x_{f(1)}$ and $x_{f(2)}$. Recall that ε_i is the energy of the initial electron in units of the threshold energy in the Breit–Wheeler process (see (16)). Let us find the values of the energy of the initial electron that it can have, so that the particles of the pair can

have energies $x_{\pm(2,4)}$. In this case, as was shown, the energy of the scattered electron has the upper bound (see Notations (28)). Let us start with the energy $x_{f(2)}$. From the Condition (28) we obtain

$$\varepsilon_i \geq \varepsilon_{thr}, \quad \varepsilon_{thr} = (1+\sqrt{2})/2 \approx 1.207. \tag{29}$$

The value ε_{thr} has the meaning of the threshold energy for the initial electron. From similar reasoning, but when considering the $x_{f(1)}$ energy of the scattered electron, one can obtain

$$\varepsilon_i \geq \varepsilon_1, \quad \varepsilon_1 = (1+\sqrt{3})/2 \approx 1.366. \tag{30}$$

In the same way, the possibilities for the particles of the pair to have energies $x_{\pm(1,3)}$ are considered . In this case, we consider the Constraint (27) first for the energy $x_{f(2)}$, which leads to the condition

$$\varepsilon_i \geq \varepsilon_2, \quad \varepsilon_2 = (2+\sqrt{6})/2 \approx 2.225 \tag{31}$$

and then for the energy $x_{f(1)}$:

$$\varepsilon_i \geq \varepsilon_3, \quad \varepsilon_3 = 1+\sqrt{2} = 2\varepsilon_{thr} \approx 2.414. \tag{32}$$

The meaning of characteristic energies $\varepsilon_{thr}, \varepsilon_1, \varepsilon_2, \varepsilon_3$ can be understood with help of Figure 3. As long as the energy of the initial electron does not exceed the value $\varepsilon_{thr} \approx 1.207$, the studied process is impossible. When the energy of the initial electron lies in the interval $\varepsilon_{thr} \approx 1.207 \leq \varepsilon_i \leq \varepsilon_1 \approx 1.366$, the energy of the scattered electron can only take values from the energy branch $x_{f(2)}$, and the energies of the pair particles can only take values $x_{\pm(2,4)}$. At this energy of the initial electron, the scattered electron cannot have energy $x_{f(1)}$, and the particles of the pair cannot have energies $x_{\pm(1,3)}$. Further, if the energy of the initial electron lies in the interval $\varepsilon_1 \approx 1.366 \leq \varepsilon_i \leq \varepsilon_2 \approx 2.225$, then the scattered electron can already have energy from any of the 2 branches $x_{f(1,2)}$, and the particles of the pair (for each of the two branches $x_{f(1,2)}$) can still have only two options for energies—$x_{\pm(2,4)}$. A more interesting situation is implemented in the energy range of the initial electron $\varepsilon_2 \approx 2.225 \leq \varepsilon_i \leq \varepsilon_3 \approx 2.414$: now, when the energy of the scattered electron from the branch $x_{f(2)}$ is implemented, the pair particles can take any of the four possible energies $x_{\pm(1,2,3,4)}$, but if the scattered electron has the energy from the branch $x_{f(1)}$, then the pair particles, as in the previous interval, can only have the energies $x_{\pm(2,4)}$. Finally, when the energy of the initial electron exceeds ε_3, that is, $\varepsilon_i \geq \varepsilon_3$, the scattered electron can have energy from either of the two branches $x_{f(1,2)}$, and the particles of the pair can also have energy with any choice of signs $x_{\pm(1,2,3,4)}$.

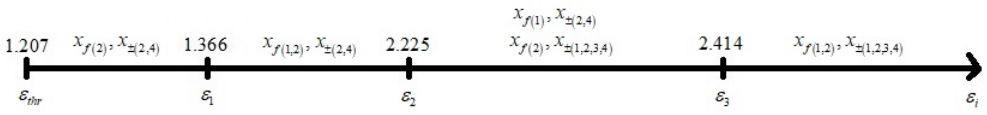

Figure 3. The regions of the initial electron energy values (in units of X-ray-stimulated Breit–Wheeler process threshold energy ω_{thr}) and the possible energies of the scattered electron and the pair particles in these regions (see Conditions (29)–(32)).

3.3. Scattered Electron Angle Bounds

Let us now consider the Condition (26) with respect to the outgoing angle of the scattered electron. The results of this investigation can be seen in Figure 4a. Consider this condition when choosing the "−" sign (solutions $x_{\pm(2,4)}$). At the energies of the initial electron $\varepsilon_{thr} \leq \varepsilon_i \leq \varepsilon_1$ we obtain that the scattered electron can only have the energy $x_{f(2)}$. In this case, its outgoing angle is limited by the value

$$\delta_{fi}^2 \leq \delta_{fi(1)}^2, \quad \delta_{fi(1)}^2 = \frac{(\varepsilon_i - (1-\sqrt{2})/2)(\varepsilon_i - \varepsilon_{thr})}{\varepsilon_i^2(\varepsilon_i - 1)^2}. \tag{33}$$

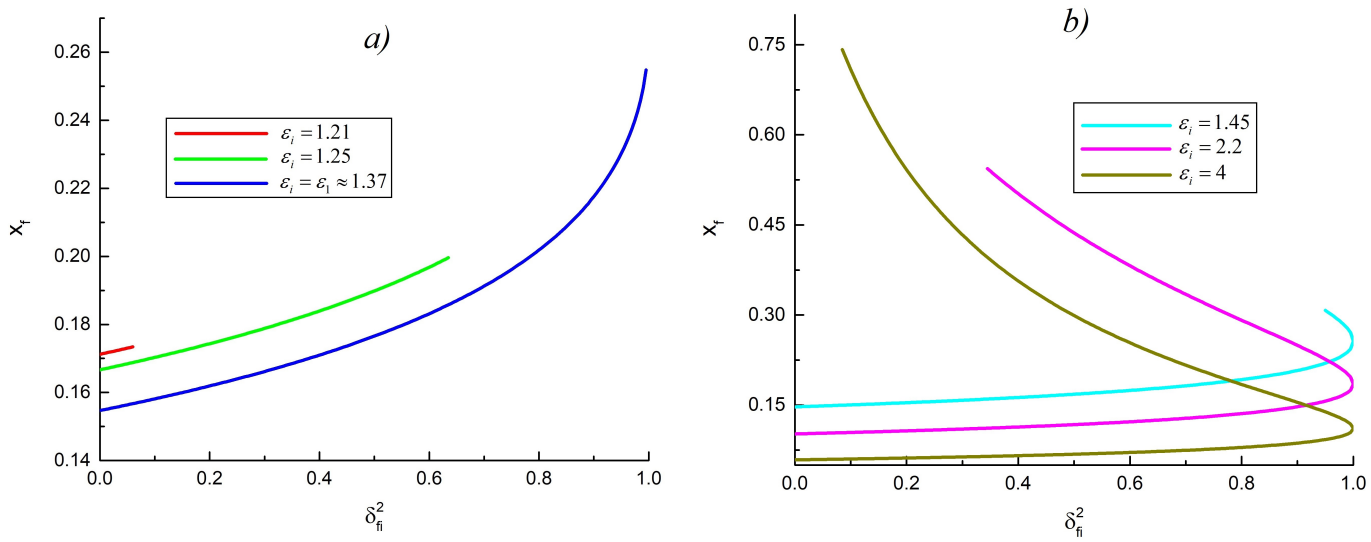

Figure 4. (**a**) The energy of the scattered electron (see Expression (17)) for different values of the energy of the initial electron from the closed interval $\varepsilon_i \in [\varepsilon_{thr} \approx 1.21, \varepsilon_1 \approx 1.37]$. (**b**) The energy of the scattered electron (see Expression (17)) for different values of the energy of the initial electron $\varepsilon_i > \varepsilon_1 \approx 1.37$.

With the energy of the initial electron $\varepsilon_i > \varepsilon_1$, when choosing the branch $x_{f(2)}$, the scattered electron can now propagate at any angle $\delta^2_{fi} \in [0, 1]$, and for the branch $x_{f(1)}$ there is a certain minimum angle (see Figure 4b):

$$\delta^2_{fi} \geq \delta^2_{fi(1)}. \tag{34}$$

We will now conduct similar to the previous point arguments, only when choosing the "+" sign (solutions $x_{\pm(1,3)}$) in Condition (26). As can be seen from the diagram in Figure 3, the solutions $x_{\pm(1,3)}$ can only be implemented when $\varepsilon_i \geq \varepsilon_2$. When the energy of the initial electron lies in the interval $\varepsilon_2 \leq \varepsilon_i \leq \varepsilon_3$, the outgoing angle of the scattered electron is not limited to 1, but to a smaller value (see Figure 4a):

$$\delta^2_{fi} \leq \delta^2_{fi(2)}, \quad \delta^2_{fi(2)} = \frac{2(\varepsilon_i - (2 - \sqrt{6})/2)(\varepsilon_i - \varepsilon_2)}{\varepsilon_i^2(\varepsilon_i - 2)^2}. \tag{35}$$

At the energy of the initial electron $\varepsilon_i > \varepsilon_3$ for the energies of the particles of the pair $x_{\pm(1,3)}$, when choosing a branch of the energy of the scattered electron $x_{f(2)}$, the scattered electron can now propagate at any angle $\delta^2_{fi} \in [0, 1]$, and for the branch $x_{f(1)}$ there is a certain minimum angle (see Figure 4b):

$$\delta^2_{fi} \geq \delta^2_{fi(2)}. \tag{36}$$

Let us now study the obtained dependencies $\delta^2_{fi(1)}(\varepsilon_i)$ and $\delta^2_{fi(2)}(\varepsilon_i)$ and what energies of the particles can be implemented in different regions of $(\varepsilon_i, \delta^2_{fi})$-space. To do this, we turn to Figure 5. In its meaning, this figure is a logical continuation and complement to the diagram shown in Figure 3.

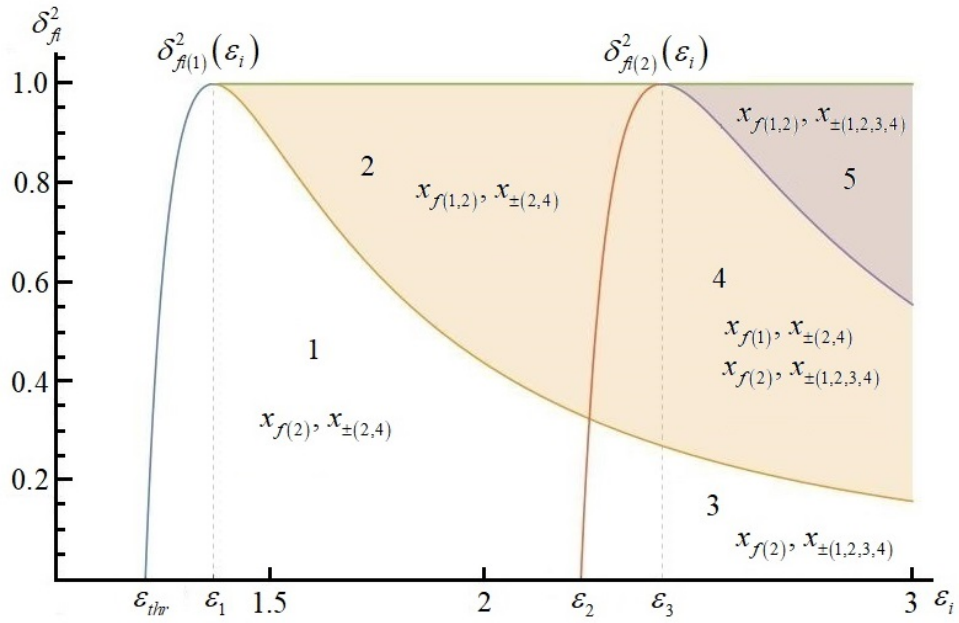

Figure 5. The dependencies of the critical angles $\delta_{fi(1)}(\varepsilon_i)$, $\delta_{fi(2)}(\varepsilon_i)$ (see Expressions (33) and (35)) on the energy of the initial electron and the regions in $(\varepsilon_i, \delta^2_{fi})$-space with different values of the particles energies allowed in them (see Conditions (33)–(36)).

Here, we describe in detail what happens in Figure 5. According to the analysis carried out above, it turns out that when studying the domain of existence of solutions $x_{\pm(2,4)}$, one needs to pay attention only to the curve $\delta^2_{fi(1)}(\varepsilon_i)$, and when studying the domain of existence of solutions $x_{\pm(1,3)}$—to the curve $\delta^2_{fi(2)}(\varepsilon_i)$. In region 1, only a branch of the energy of the scattered electron $x_{f(2)}$ and the energies of the particles of the pair $x_{\pm(2,4)}$ are possible. When the energy of the initial electron ε_i is less than the energy ε_1, the outgoing angle of the scattered electron is limited by the segment $0 \le \delta^2_{fi} \le \delta^2_{fi(1)}(\varepsilon_i)$. In region 2, when the energy of the initial electron ε_i exceeds the energy ε_1, the branch of the energy of the scattered electron $x_{f(1)}$ becomes possible. The outgoing angle of the scattered electron for the branch $x_{f(1)}$ in this case belongs to the segment $\delta^2_{fi(1)}(\varepsilon_i) \le \delta^2_{fi} \le 1$. In regions 1 and 2 when $\varepsilon_i \ge \varepsilon_1$, the scattered electron with the energy $x_{f(2)}$ can propagate at any angle $0 \le \delta^2_{fi} \le 1$. In these regions, the particles of the pair can only have energies $x_{\pm(2,4)}$. In region 3, when the energy of the initial electron ε_i exceeds the energy ε_2, it becomes possible for the particles of the pair to have energies with any signs $x_{\pm(1,2,3,4)}$. For the scattered electron, only energy $x_{f(2)}$ is available in this region. In region 4, for the energy of the scattered electron $x_{f(1)}$, as in region 2, it remains possible to be implemented if only the particles of the pair have energies $x_{\pm(2,4)}$, and also in region 4, as in region 3, for the energy of the scattered electron $x_{f(2)}$, the particles of the pair can have any energies of $x_{\pm(1,2,3,4)}$. For the energies of the initial electron ε_i exceeding the energy ε_3, a region 5 appears. In this region, the scattered electron can have any of the two energies $x_{f(1,2)}$, and also the particles of the pair can have any of the four energies $x_{\pm(1,2,3,4)}$. In regions 3 and 4, the outgoing angle of the scattered electron with the energy $x_{f(2)}$ can be any of the $0 \le \delta^2_{fi} \le 1$ for the energies of the particles of the pair $x_{\pm(2,4)}$ and is limited to the segment $0 \le \delta^2_{fi} \le \delta^2_{fi(2)}$ at the energies of the particles of the pair $x_{\pm(1,3)}$, if the energy of the initial electron lies in the segment $\varepsilon_2 \le \varepsilon_i \le \varepsilon_3$, and if $\varepsilon_i > \varepsilon_3$, then for $x_{f(2)}$ for any energies of the particles of the pair $x_{\pm(1,2,3,4)}$ the outgoing angle of the scattered electron can also be any of the segment $0 \le \delta^2_{fi} \le 1$. In regions 4 and 5, the outgoing angle of the scattered electron with the energy $x_{f(1)}$ for the energies of the particles of the pair $x_{\pm(2,4)}$ is limited by the segment $\delta^2_{fi(1)} \le \delta^2_{fi} \le 1$, and for the scattered electron with the energy $x_{f(1)}$ and the particles of the

pair with the energies $x_{\pm(1,3)}$, the outgoing angle of the scattered electron is limited by the segment $\delta^2_{fi(2)} \le \delta^2_{fi} \le 1$.

The dependencies $x_f(\delta^2_{fi})$ according to Expression (17) with Restrictions (28) taken into account are shown in Figure 4a,b.

3.4. Pair Opening Angle Bounds

Let us now analyze the Condition (26) with respect to the opening angle of the pair δ^2_{+-}. Further 2 characteristic opening angles of the pair will appear:

$$\begin{gathered}\delta^2_{+-(1,2)} = \frac{A \pm B}{\delta^4_{fi}\varepsilon^4_i}, \\ A = -2 + \delta^2_{fi}\left(2\varepsilon^2_i - 4\varepsilon_i + 1\right) + 4\delta^4_{fi}\varepsilon^2_i(\varepsilon_i - 1), \quad B = 2\left(-\varepsilon^2_i\delta^2_{fi} + 2\varepsilon_i\delta^2_{fi} + 1\right)\sqrt{1-\delta^2_{fi}}.\end{gathered} \tag{37}$$

In Expression (37) $\delta^2_{+-(1)}$ corresponds to sign "+" and $\delta^2_{+-(1)}$—to sign "−".

Let us consider the case when the particles energies take the values $x_{f(2)}$, $x_{\pm(2,4)}$. In this case, at the energies of the initial electron from the segment $\varepsilon_{thr} \le \varepsilon_i \le \varepsilon_1$, the angles change within

$$0 \le \delta^2_{fi} \le \delta^2_{fi(1)}, \quad 0 \le \delta^2_{+-} \le \delta^2_{+-(1)}. \tag{38}$$

At the energies of the initial electron from the segment $\varepsilon_1 \le \varepsilon_i \le \varepsilon_2$ we obtain the intervals of changing of the angles

$$0 \le \delta^2_{fi} \le 1, \quad 0 \le \delta^2_{+-} \le \delta^2_{+-(1)}. \tag{39}$$

When the energy of the initial electron is in the segment $\varepsilon_2 \le \varepsilon_i \le \varepsilon_3$ then

$$\begin{gathered}0 \le \delta^2_{+-} \le 1, \quad if \quad 0 \le \delta^2_{fi} \le \delta^2_{fi(2)}, \\ 0 \le \delta^2_{+-} \le \delta^2_{+-(1)}, \quad if \quad \delta^2_{fi(2)} \le \delta^2_{fi} \le 1.\end{gathered} \tag{40}$$

Finally, when energy of the initial electron satisfy the condition $\varepsilon_i > \varepsilon_3$ the angles can take any values:

$$0 \le \delta^2_{fi} \le 1, \quad 0 \le \delta^2_{+-} \le 1. \tag{41}$$

Let us now consider the case when the particles have the energies $x_{f(1)}$, $x_{\pm(2,4)}$. It should be underlined that the solution $x_{f(1)}$ exists only if the initial electron energy is greater than ε_1 (see Figure 3). If the initial electron energy is such that $\varepsilon_1 \le \varepsilon_i \le \varepsilon_3$, we have

$$\delta^2_{fi(1)} \le \delta^2_{fi} \le 1, \quad 0 \le \delta^2_{+-} \le \delta^2_{+-(2)}. \tag{42}$$

At the energies of the initial electron from the region $\varepsilon_i > \varepsilon_3$ the angles satisfy the following conditions:

$$\begin{gathered}0 \le \delta^2_{+-} \le \delta^2_{+-(2)}, \quad if \quad \delta^2_{fi(1)} \le \delta^2_{fi} \le \delta^2_{fi(2)} \\ 0 \le \delta^2_{+-} \le 1, \quad if \quad \delta^2_{fi(2)} \le \delta^2_{fi} \le 1\end{gathered} \tag{43}$$

Further we investigate the case of energies $x_{f(2)}$, $x_{\pm(1,3)}$. We underline that this case is implemented only if the energy of the initial electron is greater than ε_2 (see Figure 3). In the case $\varepsilon_2 \le \varepsilon_i \le \varepsilon_3$ the angles change in the regions

$$0 \le \delta^2_{fi} \le \delta^2_{fi(2)}, \quad \delta^2_{+-(1)} \le \delta^2_{+-} \le 1. \tag{44}$$

For the initial electron energies greater than ε_3 we obtain

$$0 \le \delta^2_{fi} \le 1, \quad 0 \le \delta^2_{+-} \le 1. \tag{45}$$

Finally, we turn to the case of the energies $x_{f(1)}$, $x_{\pm(1,3)}$. From Figure 3 it can be seen that this case is only possible when the initial electron energy is greater than ε_3. In this case we obtain

$$\delta^2_{fi(2)} \leq \delta^2_{fi} \leq 1, \quad \delta^2_{+-(2)} \leq \delta^2_{+-} \leq 1. \tag{46}$$

The results of this subsection are shown in Figures 6–8.

In Figure 6a, when the initial electron energy is $\varepsilon_{thr} \leq \varepsilon_i = 1.3 \leq \varepsilon_1$, there are only two regions: in region 1, the particles can only have energies $x_{f(2)}$, $x_{\pm(2,4)}$.

In Figure 6b, when $\varepsilon_1 \leq \varepsilon_i = 1.5 \leq \varepsilon_2$, there are already three regions: in region 1, only the energies $x_{f(2)}$, $x_{\pm(2,4)}$ are still possible, but now there appears region 2, where the particles now can have the energies $x_{f(1,2)}$, $x_{\pm(2,4)}$. There is also region 3 with no possible energies.

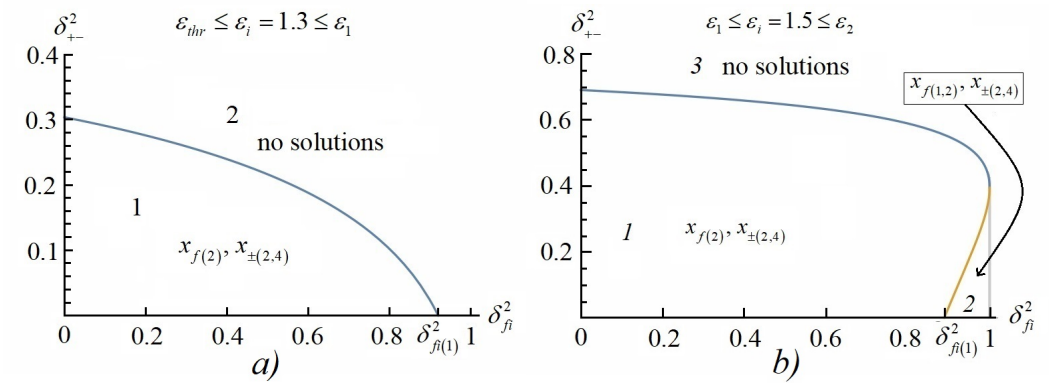

Figure 6. (**a**) Regions in $(\delta^2_{fi}, \delta^2_{+-})$–space with different possible values of particle energies. The energy of the initial electron is $\varepsilon_{thr} \leq \varepsilon_i = 1.3 \leq \varepsilon_1$ (see Condition (38)). The blue line shows the dependence of the first characteristic opening angle of the pair $\delta^2_{+-(1)}\left(\delta^2_{fi}, \varepsilon_i = 1.3\right)$ on the outgoing angle of the scattered electron at the energy of the initial electron $\varepsilon_i = 1.3$. (**b**) Regions in $(\delta^2_{fi}, \delta^2_{+-})$-space with different possible values of particle energies. The energy of the initial electron is $\varepsilon_1 \leq \varepsilon_i = 1.5 \leq \varepsilon_2$ (see Conditions (39) and (42)). The blue line shows the dependence of the first characteristic opening angle of the pair $\delta^2_{+-(1)}\left(\delta^2_{fi}, \varepsilon_i = 1.5\right)$ on the outgoing angle of the scattered electron at the energy of the initial electron $\varepsilon_i = 1.5$. The orange line shows the dependence of the second characteristic opening angle of the pair $\delta^2_{+-(2)}\left(\delta^2_{fi}, \varepsilon_i = 1.5\right)$ on the outgoing angle of the scattered electron at the energy of the initial electron $\varepsilon_i = 1.5$.

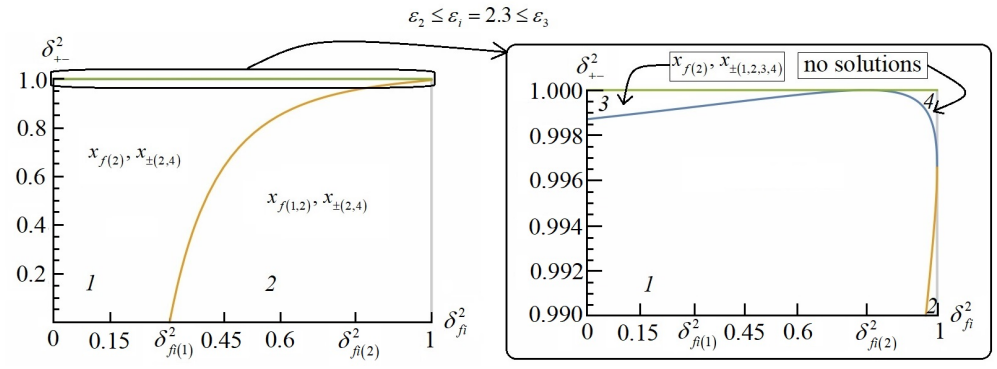

Figure 7. Regions in $(\delta^2_{fi}, \delta^2_{+-})$–space with different possible values of particle energies. The energy of the initial electron is $\varepsilon_2 \leq \varepsilon_i = 2.3 \leq \varepsilon_3$ (see Conditions (40), (42), (44)). The right picture shows the area of the left picture for $\delta^2_{+-} \in [0.99, 1]$. The blue line shows the dependence of the first characteristic opening angle of the pair $\delta^2_{+-(1)}\left(\delta^2_{fi}, \varepsilon_i = 2.3\right)$ on the outgoing angle of the scattered electron at the energy of the initial electron $\varepsilon_i = 2.3$. The orange line shows the dependence of the second characteristic opening angle of the pair $\delta^2_{+-(2)}\left(\delta^2_{fi}, \varepsilon_i = 2.3\right)$ on the outgoing angle of the scattered electron at the energy of the initial electron $\varepsilon_i = 2.3$.

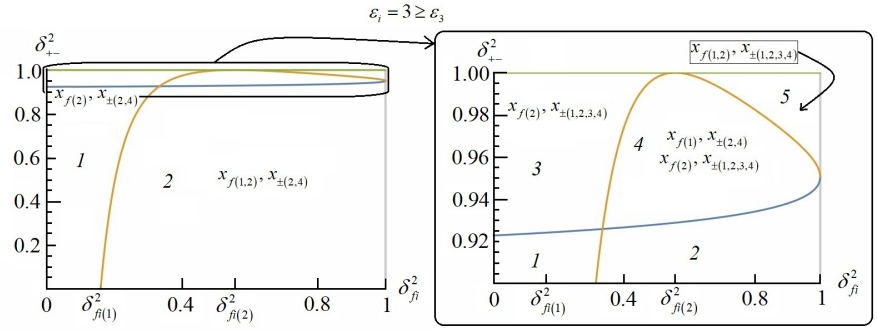

Figure 8. Regions in $(\delta^2_{fi}, \delta^2_{+-})$–space with different possible values of particle energies. The energy of the initial electron is $\varepsilon_i = 3 \geq \varepsilon_3$ (see Conditions (41), (43), (45), (46)). The right picture shows the area of the left picture for $\delta^2_{+-} \in [0.9, 1]$. The blue line shows the dependence of the first characteristic opening angle of the pair $\delta^2_{+-(1)}\left(\delta^2_{fi}, \varepsilon_i = 3\right)$ on the outgoing angle of the scattered electron at the energy of the initial electron $\varepsilon_i = 3$. The orange line shows the dependence of the second characteristic opening angle of the pair $\delta^2_{+-(2)}\left(\delta^2_{fi}, \varepsilon_i = 3\right)$ on the outgoing angle of the scattered electron at the energy of the initial electron $\varepsilon_i = 3$.

With an increase in the initial electron energy, the picture becomes more complicated. In Figure 7, for $\varepsilon_2 \leq \varepsilon_i = 2.3 \leq \varepsilon_3$, there are four distinct regions: in region 1, only the energies $x_{f(2)}$, $x_{\pm(2,4)}$ are implemented, in region 2—$x_{f(1,2)}$, $x_{\pm(2,4)}$, in region 3—$x_{f(2)}$, $x_{\pm(1,2,3,4)}$, and there is still region 4 with no solution at all.

In Figure 8, for $\varepsilon_i = 3 \geq \varepsilon_3$, there are five regions: in region 1, the particles can have only the energies $x_{f(2)}$, $x_{\pm(2,4)}$, in region 2—$x_{f(1,2)}$, $x_{\pm(2,4)}$, in region 3—$x_{f(2)}$, $x_{\pm(1,2,3,4)}$, in region 4—$x_{f(1)}$, $x_{\pm(2,4)}$ and $x_{f(2)}$, $x_{\pm(1,2,3,4)}$, and in region 5 any of the energies $x_{f(1,2)}$, $x_{\pm(1,2,3,4)}$ are possible. We underline that for the case $\varepsilon_i \geq \varepsilon_3$ there are no regions in the $\left(\delta^2_{fi}, \delta^2_{+-}\right)$–space with no solutions, that is, the particles can propagate at any angle from the square $\left(\delta^2_{fi}, \delta^2_{+-}\right) \in [0, 1] \times [0, 1]$.

Let us now have a look at the energies of the particles of the pair as functions of the angles δ^2_{fi} and δ^2_{+-} (see Expressions (23), (24), respectively). The corresponding plots can be perceived as "built over" Figures 6–8, respectively. In the interval $\varepsilon_2 \leq \varepsilon_i \leq \varepsilon_3$ for plotting the dependencies $x_\pm\left(\delta^2_{fi}, \delta^2_{+-}\right)$ (see Figure 9a,b), we take $\varepsilon_i = 2.4$, and not $\varepsilon_i = 2.3$, as in Figure 7 due to better representativeness.

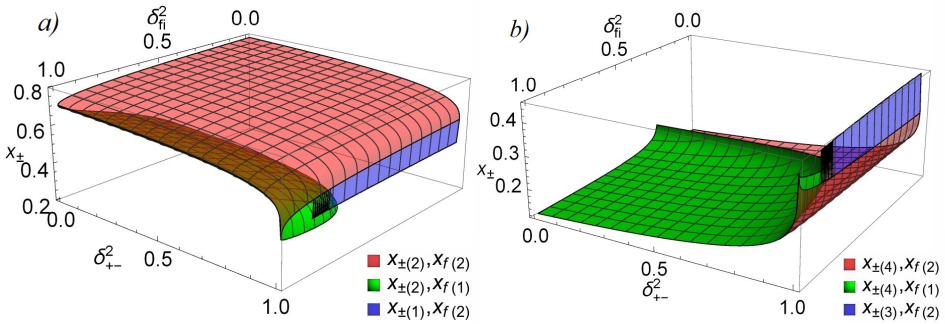

Figure 9. (**a**) The dependence of the energies of the particles of the pair $x_\pm\left(\delta^2_{fi}, \delta^2_{+-}\right)$ (see Expressions (23) and (24)) on the outgoing angle of the scattered electron and the opening angle of the pair in the energy range of the initial electron $\varepsilon_2 \leq \varepsilon_i \leq \varepsilon_3$ (see Figure 7). The figure shows the dependencies $x_{\pm(2)}$ for $x_{f(1,2)}$ and $x_{\pm(1)}$ for $x_{f(2)}$. The energy of the initial electron $\varepsilon_i = 2.4$. (**b**) The dependence of the energies of the particles of the pair $x_\pm\left(\delta^2_{fi}, \delta^2_{+-}\right)$ (see Expressions (23) and (24)) on the outgoing angle of the scattered electron and the opening angle of the pair in the energy range of the initial electron $\varepsilon_2 \leq \varepsilon_i \leq \varepsilon_3$ (see Figure 7). The figure shows the dependencies $x_{\pm(4)}$ for $x_{f(1,2)}$ and $x_{\pm(3)}$ for $x_{f(2)}$. The energy of the initial electron $\varepsilon_i = 2.4$.

4. Differential Probability per Unit Time

In this article, we will not be interested in those areas of the parameter space where channels interference is possible. The question of the existence of such areas is an independent task. Therefore, it is sufficient to consider the probability of a process occurring over a single channel. For convenience, we will consider the resonant differential probability per unit time of channel A, which is given by the expression (see formula (55) in [23])

$$dW_A = \frac{\alpha^2\eta^4}{8\pi}\frac{m^4E_i^3}{\omega_{thr}^4}\frac{x_f(1-x_f-x_+)}{x_+(1-x_f)^2}\frac{V_C U_{BW}}{B_{if}^2\left(\delta_{fi}^2-\delta_{res}^2\right)^2+\Gamma^2}dx_f d\delta_{fi}^2 d\delta_{+-}^2, \tag{47}$$

where V_C and U_{BW} are the functions that define the probabilities of the X-ray-stimulated Compton effect and the X-ray-stimulated Breit–Wheeler process, correspondingly (see [5]):

$$V_C = 2+\frac{v^2}{1+v}-\frac{4v}{v_1}\left(1-\frac{v}{v_1}\right), \quad U_{BW} = 2u-1+\frac{2u}{u_1}\left(1-\frac{u}{u_1}\right). \tag{48}$$

Relativistically invariant kinematic parameters are of the following form (see [5]):

$$u = \frac{((kp_+)+(kp_-))^2}{4(kp_+)(kp_-)} = \frac{(1-x_f)^2}{4(1-x_f-x_+)x_+}, \quad u_1 = \frac{(kp_+)+(kp_-)}{2m^2} = \varepsilon_i(1-x_f) \tag{49}$$

and

$$vs. = \frac{(kp_i)-(kp_f)}{(kp_f)} = \frac{1-x_f}{x_f}, \quad v_1 = \frac{2(kp_i)}{m^2} = 4\varepsilon_i. \tag{50}$$

In Expression (47)

$$\begin{aligned} B_{if} &= \frac{2m^2\varepsilon_i^2 x_f}{E_i(1-x_f)}, \quad \Gamma = \frac{W_C}{2}, \quad W_C = \frac{\alpha m^2}{32\pi E_i}\eta^2 W', \\ W' &= \left(1-\frac{4}{v_1}-\frac{8}{v_1^2}\right)\ln(1+v_1)+\frac{1}{2}+\frac{8}{v_1}-\frac{1}{2(1+v_1)^2}. \end{aligned} \tag{51}$$

In Expression (51) Γ is the width of the resonance resulting from the application of the Breit–Wigner procedure and W_C - is the total probability per unit time of the X-ray-stimulated Compton effect. The factor $\left(\delta_{fi}^2-\delta_{res}^2\right)^2$ in the denominator describes the difference between actual outgoing angle of the scattered electron and its resonance value. Under the resonance condition, when $\delta_{fi}^2=\delta_{res}^2$, the differential probability per unit time (47) reaches its maximum value

$$\frac{dW_A^{max}}{dx_f d\delta_{fi}^2 d\delta_{+-}^2} \approx \alpha^2 m F\left(\delta_{fi}^2,\delta_{+-}^2\right) \sim \frac{dW_{nonres}}{dx_f d\delta_{fi}^2 d\delta_{+-}^2}F\left(\delta_{fi}^2,\delta_{+-}^2\right), \tag{52}$$

where

$$F\left(\delta_{fi}^2,\delta_{+-}^2\right) = \frac{512\pi}{\alpha^2}\frac{E_i}{m}\left(\frac{E_i}{\omega_{thr}}\right)^4\frac{x_f(1-x_f-x_+)}{x_+(1-x_f)^2}\frac{V_C U_{BW}}{W'^2} \tag{53}$$

and dW_{nonres} denotes the non-resonant differential probability per unit time, the value of which is determined by the Expression (47) far from the resonance $\left(B_{if}^2\left(\delta_{fi}^2-\delta_{res}^2\right)^2 \gg \Gamma^2\right)$.

For an X-ray pulsar with a frequency $\omega = 1$ keV the threshold energy is $\omega_{thr} \sim 1$ GeV. To obtain positrons with energies of order of 100 GeV discussed in [28], it is necessary to have the initial electron of at least the same energy that corresponds to $\varepsilon_i = 100$. The resonant differential probability per unit time of the process in channel A in units $\alpha^2 m$ (see Expression (52)) for the case when the energy of the resulting positron differs slightly from the energy of the initial electron is shown in Figure 10a. High-energy positrons

correspond to solutions $x_{+(1,2)}$, $x_{f(1,2)}$ at not too small scattering angles of the electron and opening angles of the pair. For these four solutions, the resonant differential probabilities per unit time differ slightly from each other (by less than an order of magnitude) and behave in a similar way, so we give only the resonant differential probability per unit time for the case $x_{+(1)}$, $x_{f(1)}$ (see Figure 10b). As can be seen from Expression (52) and from Figure 10a, as the positron energy increases, the resonant differential probability probability of such a process decreases significantly.

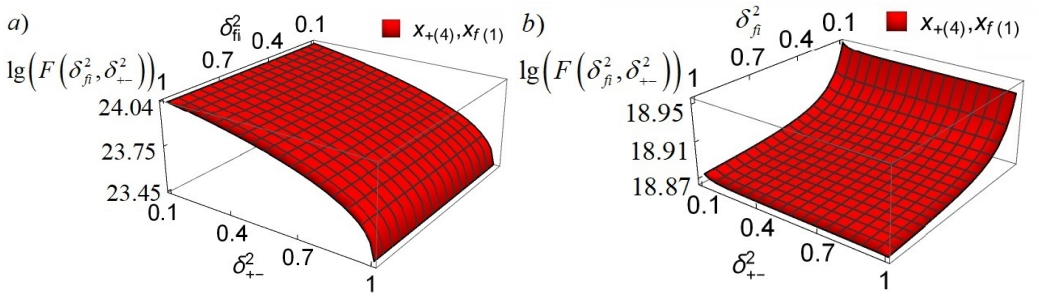

Figure 10. (**a**) The angular distribution of the resonant differential probability per unit time of the process (see Expression (52)) for positrons with the energies $x_{+(4)}$ for $x_{f(1)}$. The energy of the field quanta $\omega = 1$ keV, the energy of the initial electron $E_i = 100$ GeV, the initial electron propagates towards the X-ray wave. (**b**) The angular distribution of the resonant differential probability per unit time of the process (see Expression (52)) for high-energy positrons $x_{+(1)}$ for $x_{f(1)}$ with the energies similar to the initial electron energy. The energy of the field quanta $\omega = 1keV$, the energy of the initial electron $E_i = 100$ GeV, the initial electron propagates towards the X-ray wave.

The maximum value of the resonant differential probability per unit time of the process, which corresponds to $x_{+(4)}$, is 24 orders greater than the non-resonant differential probability per unit time (see Figure 10a). In the case of high-energy positrons $x_{+(1)}$ the resonant differential probability per unit time of the process reaches a value of 19 orders of the value of the non-resonant differential probability per unit time (see Figure 10b), which is less than the maximum value for this process, but still much greater than the differential probability per unit time of the non-resonant process.

5. Conclusions

The kinematics of resonant electron-positron pairs production in collision of high-energy electrons with a low-intensity (see Condition (3)) X-ray field was studied. Expressions were obtained for the energies of the outgoing particles, which essentially depend on the outgoing angle of the scattered electron and the opening angle of the pair (see Expressions (17), (23) and (24), as well as and Figures 4 and 11–13). According to these expressions, at fixed angles δ_{fi}^2 and δ_{+-}^2 up to eight different values of the particles energies of the pair are possible. Except for the regions with eight different energies of the particles of the pair (region 5 in Figure 8) there are regions with six different energies (region 4 in Figure 8), four different energies (region 2 in Figure 6b regions 2 and 3 in Figures 7 and 8), two different energies (regions 1 in Figures 6–8) and no solutions at all (region 2 in Figure 6a, region 3 in Figure 6b and region 4 in Figure 7). When the energy of the initial electron is high enough (see Condition (32)) there are at least two different energies of the particles of the pair at any outgoing angle of the scattered electron and opening angle of the pair.

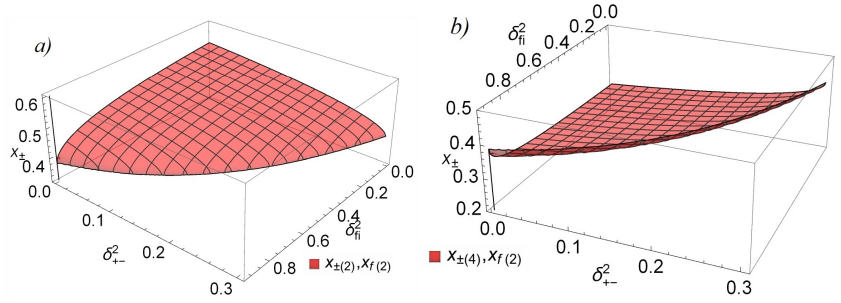

Figure 11. (**a**) The dependence of the energies of the particles of the pair $x_{\pm}\left(\delta^2_{fi}, \delta^2_{+-}\right)$ (see Expressions (23) and (24)) on the outgoing angle of the scattered electron and the opening angle of the pair in the energy range of the initial electron $\varepsilon_{thr} \leq \varepsilon_i \leq \varepsilon_1$ (see Figure 6a). The figure shows the dependence $x_{\pm(2)}$ for $x_{f(2)}$. The energy of the initial electron $\varepsilon_i = 1.3$. (**b**) The dependence of the energies of the particles of the pair $x_{\pm}\left(\delta^2_{fi}, \delta^2_{+-}\right)$ (see Expressions (23) and (24)) on the outgoing angle of the scattered electron and the opening angle of the pair in the energy range of the initial electron $\varepsilon_{thr} \leq \varepsilon_i \leq \varepsilon_1$ (see Figure 6a). The figure shows the dependence $x_{\pm(4)}$ for $x_{f(2)}$. The energy of the initial electron $\varepsilon_i = 1.3$.

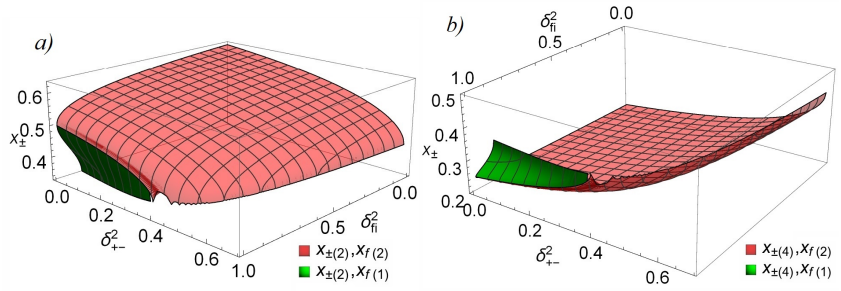

Figure 12. (**a**) The dependence of the energies of the particles of the pair $x_{\pm}\left(\delta^2_{fi}, \delta^2_{+-}\right)$ (see Expressions (23) and (24)) on the outgoing angle of the scattered electron and the opening angle of the pair in the energy range of the initial electron $\varepsilon_1 \leq \varepsilon_i \leq \varepsilon_2$ (see Figure 6b). The figure shows the dependencies $x_{\pm(2)}$ for $x_{f(1,2)}$. The energy of the initial electron $\varepsilon_i = 1.5$. (**b**) The dependence of the energies of the particles of the pair $x_{\pm}\left(\delta^2_{fi}, \delta^2_{+-}\right)$ (see Expressions (23) and (24)) on the outgoing angle of the scattered electron and the opening angle of the pair in the energy range of the initial electron $\varepsilon_1 \leq \varepsilon_i \leq \varepsilon_2$ (see Figure 6b). The figure shows the dependencies $x_{\pm(4)}$ for $x_{f(1,2)}$. The energy of the initial electron $\varepsilon_i = 1.5$.

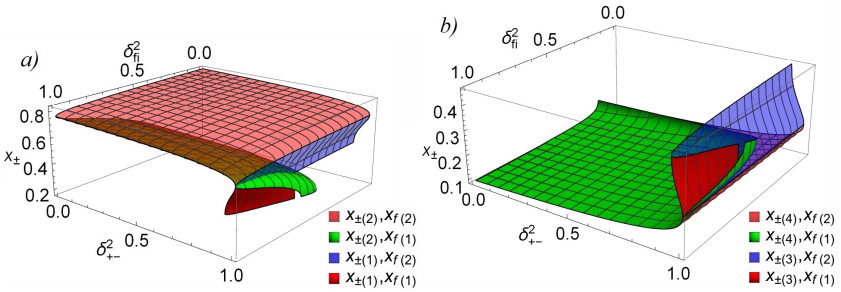

Figure 13. (**a**) The dependence of the energies of the particles of the pair $x_{\pm}\left(\delta^2_{fi}, \delta^2_{+-}\right)$ (see Expressions (23) and (24)) on the outgoing angle of the scattered electron and the opening angle of the pair in the energy range of the initial electron $\varepsilon_i \geq \varepsilon_3$ (see Figure 8). The figure shows the dependencies $x_{\pm(1,2)}$ for $x_{f(1,2)}$. The energy of the initial electron $\varepsilon_i = 3$. (**b**) The dependence of the energies of the particles of the pair $x_{\pm}\left(\delta^2_{fi}, \delta^2_{+-}\right)$ (see Expressions (23) and (24)) on the outgoing angle of the scattered electron and the opening angle of the pair in the energy range of the initial electron $\varepsilon_i \geq \varepsilon_3$ (see Figure 8). The figure shows the dependencies $x_{\pm(3,4)}$ for $x_{f(1,2)}$. The energy of the initial electron $\varepsilon_i = 3$.

The kinematic constraints on the energies of the scattered electron (see Expressions (27) and (28) and Figure 2) was investigated. In particular, the scattered electron energy has the top bound $x^2_{f;max} \leq 1 - 1/\varepsilon_i$. There is also a characteristic energy of the scattered electron (see Expression (27)) which is that in the case scattered electron having greater energy then up to 8 different energy values are possible for the particles of the pair to have, and in other case they can have only up to four different energies. The initial electron energy has the threshold value (see Expression (29)) and three more characteristic values (see Expressions (30)–(32), also Figure 3)), which are of the similar meaning as the characteristic energy of the scattered electron—the higher the energy of the initial electron (compared to the characteristic energies) the higher the possibility for the particles of the pair to have up to eight different energies.

The angles space was investigated thoroughly. The characteristic values for the outgoing angle of the scattered electron and opening angle of the pair (see Expressions (33), (35) and (37)) were found. These curves in the angles space divide it into several regions with different number of distinct possible energies of the particles (see Figures 5, 6 and 8). These regions and the number of possible energies in them are discussed in detail (see Sections 3.3 and 3.4).

Resonant differential probability per unit time of the process was obtained (see Expression (52) and Figure 10). In general, the resonant differential probability per unit time is rather weakly dependent on the angles: with an increase in the opening angle of the pair, the probability decreases slightly. The resonant differential probability per unit time reaches its maximum, which is 24 orders higher than the non-resonant differential probability per unit time, for low-energy positrons $x_{+(4)}$ (see Figure 10a), and for high-energy positrons, in which case we are more interested, it decreases to a maximum value of order of 19 orders of the value of the non-resonant differential probability per unit time, which is still munch greater than the value of the non-resonant differential probability per unit time (see Figure 10b).

Author Contributions: Conceptualization, S.P.R.; methodology, S.P.R. and V.V.D.; software, G.K.S.; validation, S.P.R., V.V.D. and G.K.S.; formal analysis, S.P.R. and G.K.S.; investigation, S.P.R., V.V.D. and G.K.S.; resources, V.V.D.; data curation, S.P.R. and V.V.D.; writing—original draft preparation, G.K.S.; writing—review and editing, S.P.R. and G.K.S.; visualization, G.K.S.; supervision, S.P.R. and V.V.D.; project administration, V.V.D.; funding acquisition, V.V.D. All authors have read and agreed to the published version of the manuscript.

Funding: This research received no external funding.

Institutional Review Board Statement: Not applicable.

Informed Consent Statement: Not applicable.

Conflicts of Interest: The authors declare no conflict of interest.

References

1. Oleinik, V. Resonance Effects in the Field of an Intense Laser Beam. *J. Exp. Theor. Phys.* **1967**, *25*, 697.
2. Oleinik, V. Resonance Effects in the Field of an Intense Laser Ray. *J. Exp. Theor. Phys.* **1968**, *26*, 1132.
3. Roshchupkin, S.P. Resonant Effects in Collisions of Relativistic Electrons in the Field of a Light Wave. *Laser Phys.* **1996**, *6*, 837–858.
4. Roshchupkin, S.P.; Lebed', A.A.; Padusenko, E.A.; Voroshilo, A.I. Resonant effects of quantum electrodynamics in the pulsed light field. In *Quantum Optics and Laser Experiments*; Intech: Croatia, Rijeka, 2012; Chapter 6, pp. 107–156.
5. Ritus, V.I.; Nikishov, A.I. Quantum Electrodynamics Phenomena in the Intense Field. *Trudy FIAN* **1979**, *111*.
6. Roshchupkin, S. Resonant Electron-Electron Scattering in the Field of a Light Wave: The General Relativistic Case. *Laser Phys.* **1994**, *4*, 139–147.
7. Voroshilo, O.; Roshchupkin, S. Resonant two-photon emission of an electron in the field of an electromagnetic wave. *Voprosy Atomnoj Nauki i Techniki = Pytannja Atomnoĭ Nauky i Techniky = Probl. At. Sci. Technol.* **2007**, *3*, 221–224. Available online: http://dspace.nbuv.gov.ua/handle/123456789/110951 (accessed on 22 June 2021).
8. Roshchupkin, S.P.; Lebed', A.A. *Effects of Quantum Electrodynamics in the Strong Pulsed Laser Fields*; Naukova Dumka: Kiev, Ukraine, 2013.

9. Roshchupkin, S.P. Resonant Spontaneous Bremsstrahlung of an Electron in the Field of the Nucleus and Two Light Waves. *Laser Phys.* **2002**, *12*, 498–503.
10. Voroshilo, A.I.; Roshchupkin, S.P. Resonant scattering of a photon by an electron in the field of a circularly polarized electromagnetic wave. *Laser Phys. Lett.* **2005**, *2*, 184–189. [CrossRef]
11. Voroshilo, A.; Roshchupkin, S.; Denisenko, O. Resonance of exchange amplitude of Compton effect in the circularly polarized laser field. *Eur. Phys. J. D* **2007**, *41*, 433–440. [CrossRef]
12. Lebed', A.A.; Roshchupkin, S.P. Resonant spontaneous bremsstrahlung by an electron scattered by a nucleus in the field of a pulsed light wave. *Phys. Rev. A* **2010**, *81*, 033413. [CrossRef]
13. Nedoreshta, V.; Voroshilo, A.; Roshchupkin, S. Resonant scattering of an electron by a muon in the field of light wave. *Eur. Phys. J. D* **2008**, *48*, 451–458. [CrossRef]
14. Larin, N.R.; Dubov, V.V.; Roshchupkin, S.P. Resonant production of electron-positron pairs by a hard gamma-ray on a nucleus in an external electromagnetic field. *Mod. Phys. Lett. A* **2020**, *35*, 2040025. [CrossRef]
15. Dubov, A.; Dubov, V.; Roshchupkin, S. Resonant emission of hard gamma-quanta at scattering of ultrarelativistic electrons on a nucleus within the external light field. *Mod. Phys. Lett. A* **2020**, *35*, 2040024. [CrossRef]
16. Doroshenko, D.; Dubov, V.; Roshchupkin, S. Resonant annihilation and production of high-energy electron-positron pairs in an external electromagnetic field. *Mod. Phys. Lett. A* **2020**, 2040023. [CrossRef]
17. Nedoreshta, V.N.; Roshchupkin, S.P.; Voroshilo, A.I. Resonance of the exchange amplitude of a photon by an electron scattering in a pulsed laser field. *Phys. Rev. A* **2015**, *91*, 062110. [CrossRef]
18. Nedoreshta, V.N.; Voroshilo, A.I.; Roshchupkin, S.P. Resonant scattering of a photon by an electron in the moderately-strong-pulsed laser field. *Phys. Rev. A* **2015**, *88*, 052109. [CrossRef]
19. Larin, N.R.; Dubov, V.V.; Roshchupkin, S.P. Resonant photoproduction of high-energy electron-positron pairs in the field of a nucleus and a weak electromagnetic wave. *Phys. Rev. A* **2019**, *100*, 052502. [CrossRef]
20. Dubov, A.; Dubov, V.V.; Roshchupkin, S.P. The Resonant Bremsstrahlung of Ultrarelativistic Electrons on a Nucleus with Radiation of Hard Gamma-Quanta in the Presence of a Pulsed Field of the X-ray Pulsar. *Universe* **2020**, *6*, 143. [CrossRef]
21. Larin, N.R.; Roshchupkin, S.P.; Dubov, V.V. Resonant Effects in a Photoproduction of Ultrarelativistic Electron-Positron Pairs on a Nucleus in the Field of the X-ray Pulsar. *Universe* **2020**, *6*, 141. [CrossRef]
22. Doroshenko, D.V.; Roshchupkin, S.P.; Dubov, V.V. The Resonant Effect of an Annihilation Channel in the Interaction of the Ultrarelativistic Electron and Positron in the Field of an X-ray Pulsar. *Universe* **2020**, *6*, 137. [CrossRef]
23. Sizykh, G.K.; Roshchupkin, S.P.; Dubov, V.V. Resonant Ultrarelativistic Electron–Positron Pair Production by High-Energy Electrons in the Field of an X-ray Pulsar. *Universe* **2020**, *6*, 132. [CrossRef]
24. Roshchupkin, S.P.; Dubov, A.; Dubov, V.V. Resonant effects in the spontaneous bremsstrahlung process of ultrarelativistic electrons in the fields of a nucleus and a pulsed light wave. *Laser Phys. Lett.* **2021**, *18*, 045301. [CrossRef]
25. Roshchupkin, S.P.; Larin, N.R.; Dubov, V.V. Resonant effect of the ultrarelativistic electron–positron pair production by gamma quanta in the field of a nucleus and a pulsed light wave. *Laser Phys.* **2021**, *31*, 045301. [CrossRef]
26. Dubov, A.; Dubov, V.V.; Roshchupkin, S.P. Resonant high-energy bremsstrahlung of ultrarelativistic electrons in the field of a nucleus and a weak electromagnetic wave. *Laser Phys. Lett.* **2020**, *17*, 045301. [CrossRef]
27. Hooper, D.; Blasi, P.; Serpico, P.D. Pulsars as the sources of high energy cosmic ray positrons. *J. Cosmol. Astropart. Phys.* **2009**, *2009*, 025. [CrossRef]
28. Adriani, O.; Barbarino, G.C.; Bazilevskaya, G.A.; Bellotti, R.; Boezio, M.; Bogomolov, E.A.; Bonechi, L.; Bongi, M.; Bonvicini, V.; Bottai, S.; et al. An anomalous positron abundance in cosmic rays with energies 1.5–100 GeV. *Nature* **2009**, *458*, 607–609. [CrossRef] [PubMed]
29. Mackenroth, F.; Di Piazza, A. Nonlinear trident pair production in an arbitrary plane wave: A focus on the properties of the transition amplitude. *Phys. Rev. D* **2018**, *98*, 116002. [CrossRef]
30. Dinu, V.; Torgrimsson, G. Trident pair production in plane waves: Coherence, exchange, and spacetime inhomogeneity. *Phys. Rev. D* **2018**, *97*, 036021. [CrossRef]
31. Hu, H.; Müller, C.; Keitel, C.H. Complete QED Theory of Multiphoton Trident Pair Production in Strong Laser Fields. *Phys. Rev. Lett.* **2010**, *105*, 080401. [CrossRef]
32. Bula, C.; McDonald, K.T.; Prebys, E.J.; Bamber, C.; Boege, S.; Kotseroglou, T.; Melissinos, A.C.; Meyerhofer, D.D.; Ragg, W.; Burke, D.L.; et al. Observation of Nonlinear Effects in Compton Scattering. *Phys. Rev. Lett.* **1996**, *76*, 3116–3119. [CrossRef]
33. Ilderton, A. Trident Pair Production in Strong Laser Pulses. *Phys. Rev. Lett.* **2011**, *106*, 020404. [CrossRef]
34. King, B.; Ruhl, H. Trident pair production in a constant crossed field. *Phys. Rev. D* **2013**, *88*. [CrossRef]
35. Berestetskii, V.B.; Pitaevskii, L.P.; Lifshitz, E.M. *Quantum Electrodynamics*; Butterworth-Heinemann: Oxford, UK, 1982.
36. Roshchupkin, S.P.; Tsybul'nik, V.A.; Chmirev, A.N. The Probability of Multiphoton Processes in Quantum Electrodynamics Phenomena in a Strong Light Field. *Laser Phys.* **2000**, *10*, 1231–1248.